Development of a method for determining the relevant geomechanical parameters for evaluating the hydraulic erodibility of rock

Lamine Boumaiza[a]*, Ali Saeidi[a], and Marco Quirion[b]

[a]*Département des Sciences appliquées, Université du Québec à Chicoutimi, Chicoutimi (Québec), G7H 2B1, Canada*

[b]*Expertise en barrages, Direction Barrages et infrastructures, Hydro-Québec, Montréal, (Québec), H2Z 1A4, Canada*

*Corresponding author: E-mail address: lamine.boumaiza@uqac.ca (L. Boumaiza)

Abstract

Among the methods used for evaluating the potential hydraulic erodibility of rock, the most common are those based on the correlation between the force of flowing water and the capacity of a rock to resist erosion, such as Annandale's and Pells's methods. The capacity of a rock to resist erosion is evaluated based on erodibility indices that are determined from specific geomechanical parameters of a rock mass. These indices include the unconfined compressive strength of rock, rock block size, joint shear strength, a block's shape and orientation relative to the direction of flow, joint openings, and the nature of the surface to be potentially eroded. However, it is difficult to determine the relevant geomechanical parameters for evaluating the hydraulic erodibility of rock. The assessment of eroded unlined spillways of dams has shown that the capacity of a rock to resist erosion is not accurately evaluated. Using more than 100 case studies, we develop a method to determine the relevant geomechanical parameters for evaluating the hydraulic erodibility of rock in unlined spillways. The unconfined compressive strength of rock is found not to be relevant parameter for evaluating the hydraulic erodibility of rock. On the other hand, we find that the use of three-dimensional block volume measurements, instead of the block size factor used in Annandale's method, improves the rock block size estimation. Furthermore, the parameter representing the effect of a rock block's shape and orientation relative to the direction of flow, as considered in Pells's method, is more accurate than the parameter adopted by Annandale's method.

Keywords: Rock mass, Hydraulic erodibility, Geomechanical parameters, Rock block size, Annandale's method, Pells's method, Kirsten's index, Erosion level

Symbol notation list

a_1: Longest dimension of a rock block (m)
a_3: Shortest dimension of a rock block (m)
D_i: Erosion level
E_{doa}: Erosion, discontinuity orientation adjustment
eGSI: Erodibility geological strength index
GSI: Geological strength index
i: Erosion level class
J_a: Joint surface alteration number
J_n: Joint set number
J_o: Joint opening (mm)
J_r: Joint roughness number
J_s: Relative block structure
Jv: Number of joints intersecting a volume of 1 m^3
K_b: Rock block size number
K_d: Joint shear strength number
LF: Likelihood factor
M_s: Compressive strength number
N: Kirsten's index
n_i: Number of study cases of a given erosion level
NPES: Nature of the potentially eroding surface
n_t: Total number of study cases
P_a: Available hydraulic stream power (kW/m^2)
P_i: Probability of erosion
RF: Relative importance factor
RMR: Rock mass rating system
RMEI: Rock mass erosion index
RMi: Rock mass index
RMSE: Root mean square error (%)
RQD: Rock quality designation
Sa: Average joint spacing (m)
S_1: Spacing in joint set (m)
UCS: Unconfined compressive strength (MPa)
μ_D: Mean erosion level for a given hydraulic steam power category
V_b: Rock block volume (m^3)
γ_1: Angles between joint sets (°)
β: Block shape factor
λ_n: Joint frequency

1 Introduction

Many rock mass classification systems used in engineering were developed during the last century. The most common are the rock mass rating (*RMR*) system (Bieniawski, 1973), the Q-system, also known as the Norwegian Geotechnical Institute classification (Barton et al., 1974), the geological strength index (*GSI*) proposed by Hoek et al. (1995), and the rock mass index (*RMi*) system (Palmstrom, 1996). These classification systems were developed for multiple purposes, including underground excavation stability and support design. Furthermore, some have been used to develop related indices to evaluate the excavatability of earth materials, such as Weaver's classification (Weaver, 1975), which was based on the *RMR* system, and Kirsten's index (Kirsten, 1982), which includes several of parameters used in the Q-system.

During the Cincinnati Symposium (Kirkaldie, 1988) that focused on engineering rock mass classification systems, it was proposed that the mechanical excavatability and the hydraulic erodibility of earth materials could be considered as similar processes (Moore and Kirsten 1988). Van Svhalkwyk (1989), Pitsiou (1990), and Moore (1991) then demonstrated that the existing rock mass classification systems used for evaluating the mechanical excavatability of rock incorporate most of parameters that affect the hydraulic erodibility of rock. The term " erodibility " is used here to describe significant localized erosion of rock that occurs when the rock is submitted to hydraulic erosive power. Van Schalkwyk et al. (1994) tested several rock mass characterization indices for evaluating the hydraulic erodibility of rock, and they found that the indices generated similar results. However, Kirsten's index is more accurate (Pells, 2016a). This index, initially developed to evaluate the excavatability of earth materials, has since been adopted for assessing the hydraulic erodibility of earth materials where the "direction of excavation" of the original index has been replaced by the "direction of flow"

(Annandale, 2006, 1995; Annandale and Kirsten, 1994; Doog, 1993; Kirsten et al., 2000; Pitsiou, 1990; Van Schalkwyk et al., 1994). In these cited works, the assessment of hydraulic erodibility is based on a correlation between the erosive force of flowing water and the capacity of the rock to resist the erosive force[1]. The erosive force of flowing water is the hydraulic energy, expressed in kW/m^2, generated by the flowing water. This erosive force is usually called the available hydraulic stream power (P_a). For its part, the resistance capacity of rock can be evaluated using the Kirsten's index (Kirsten, 1988, 1982), which is determined according to certain geomechanical factors related to the intact rock and the rock mass, such as the unconfined compressive strength (*UCS*) of rock (M_s), the rock block size (K_b), the joint shear strength (K_d), and the relative block structure (J_s), which considers the effect of a block's shape and orientation relative to the direction of excavation. Kirsten's index (N) can be calculated according to Eq. (1):

$$N = M_s \cdot K_b \cdot K_d \cdot J_s \tag{1}$$

Although there are several developed methods using this correlation approach, Annandale's method (Annandale, 2006, 1995) is the most common (Castillo and Carrillo, 2016; Hahn and Drain, 2010; Laugier et al., 2015; Mörén and Sjöberg, 2007; Pells et al., 2015; Rock, 2015), and this method has been validated in a series of laboratory tests (Annandale et al., 1998; Kuroiwa et al., 1998; Wittler et al., 1998). Recently, Pells (2016a) proposed two other indices to assess the capacity of rock to resist flowing water. The first, *eGSI*, represents a modification of *GSI* previously proposed by Hoek et al. (1995) to characterize the rock mass environment. When the *GSI* index is determined using the *RMR* system, the discontinuity orientation factor is removed from *RMR* (Bieniawski, 1976). Pells (2016a) proposed the *eGSI* index to include a

[1] As noted in Pells (2016a), methods to characterize the "erosive capacity" of a flow and relate it to the "erosive resistance" of the earth or rock material date back many centuries; Rouse and Ince (1957) provide evidence of such a pursuit by Domenico Guglielmini in 1697.

new discontinuity orientation adjustment factor (E_{doa}) to represent the effect of a rock block's shape and orientation relative to the direction of flow (Eq. 2).

$$eGSI = GSI + E_{doa} \tag{2}$$

The second index proposed by Pells (2016a) is the *RMEI* (rock mass erosion index). It can be determined based on the relative importance factor (RF) and likelihood factor (LF) as presented in Eq. (3). The prefixes P1 to P5 in Eq. (3) are various sets of parameters that represent, respectively, the kinematically viable mechanism for detachment, the nature of the potentially eroding surface, the nature of the defects, the spacing of the basal defect, and the block shape (Pells 2016a).

$$RMEI = (RF_{P1}.LF_{P1}).(RF_{P2}.LF_{P2}).[(RF_{P3}.LF_{P3})+(RF_{P4}.LF_{P4})+(RF_{P5}.LF_{P5})] \tag{3}$$

Bieniawski (1973) showed that rock mass strength is controlled mostly by joint intensity and joint spacing. Even though the rock substance itself may be strong, impermeable, or both, systems of joints create significant weaknesses and favor fluid conductivity (Goodman 1993). Boumaiza et al. (2017) argued that the *UCS* of rock could beget a less important impact on the shifting-up of erodibility class. Pells (2016a) considered that the *UCS* of rock plays a very limited role in the erodibility of fractured rock masses. For example, spectacular erosion events occurred in rock having high *UCS* values at Copeton Dam in Australia, where a 20 m deep erosion gully was formed, and at the Mokolo Dam in South Africa, where a 30 m deep erosion gully was produced (Pells, 2016a). However, compared to other considered parameters, Kirsten's index is determined to a great extent by the *UCS* rating having values ranging from 0.87 to 280 MPa.

Pells et al. (2017a) argued that at the time of its development, the *RQD* (rock quality designation) parameter, used as a part of the K_b factor, was developed for a specific application

and that this parameter is sometimes applied inconsistently in practice. Accordingly, Pells (2016a) recommends use of the Marinos & Hoek (2000) chart to determine *GSI* (also used to determine the *eGSI* index), as it does not consider the *UCS* of the rock nor the *RQD*. However, this chart remains semi-qualitative, and any subsequent evaluation can be greatly influenced by the judgment of the analyst. Furthermore, it was not developed to assess the hydraulic erodibility of rock. It does not incorporate details on joint openings (J_o) that can play a determining role in the hydraulic erodibility process. Pells (2016a) included J_o and other geological parameters, such as the nature of the potentially eroding surface (*NPES*), within the *RMEI* classification. *NPES* is deemed as an important parameter in *RMEI* classification, more so than other considered parameters, such as joint spacing and block shape (Pells 2016a). Nonetheless, these existing rock mass indices fail to represent the mechanisms of erosion observed in field investigations.

The J_s parameter included in Kirsten's index is mathematically quantified based on the effect of a block's shape and orientation relative to the direction of excavation. This parameter was, furthermore, adopted by other systems developed to evaluate the excavatability of earth materials (Scoble et al. 1987, Hadjigeorgiou and Poulin 1998). Pells (2016a) argued, based on the field observations of multiple eroded spillways and laboratory experiments, that the J_s values proposed by Kirsten (1982) for assessing mechanical excavatability of earth materials are not intuitively representative of an assessment of hydraulic erodibility. Furthermore, as set by Kirsten, its rating from 0.37–1.5 has only a subtle impact on the value of Kirsten's index compared to the *UCS* rating of rock that ranges from 0.87–280. For this purpose, Pells (2016a) proposed the E_{doa} factor to represent the effect of the block's shape and orientation relative to the direction of hydraulic flow. Palmstrom et al. (2002), discussing the limitations of the Q-

system (Barton et al., 1974), argued that the block size factor K_b, which is included in Kirsten's index, provides no meaningful quantification of rock block size. Accordingly, Palmstrom (2005) and Palmstrom and Broch (2006) stated that using block volume (V_b) instead of the K_b parameter would improve the quality of Q-system results. Grenon and Hadjigeorgiou (2003) have also concluded, from in-situ investigations in Canadian mines, that K_b is an inaccurate parameter for characterizing block size.

In summary, the key geomechanical parameters to be used for assessing the hydraulic erodibility of rock remain uncertain. The *UCS* of rock, favored by Kirsten (1982) as a relevant parameter of rock mass competence, is deemed as being less relevant by Pells (2016a) and others. The K_b parameter used in Kirsten's index as an indication of block size is also deemed as inappropriate by some, including Grenon and Hadjigeorgiou (2003). Although J_o could have an important role in the assessment of the hydraulic erodibility of rock, this parameter was not considered directly by Kirsten's index, and it was ignored completely by the *eGSI* index when *GSI* is determined using Marinos & Hoek's (2000) chart. As well, values for the J_s parameter, as proposed by Kirsten (1982) for assessing the mechanical excavatability of earth materials, are seen by Pells (2016a) as having no intuitively representative values for assessing hydraulic erodibility. Furthermore, *NPES* is deemed to be a relevant parameter for evaluating the hydraulic erodibility of rock. In short, there exists no clear consensus on what geomechanical parameters are indeed relevant for evaluating the hydraulic erodibility of rock.

This paper presents a method for determining the relevant geomechanical parameters when evaluating the hydraulic erodibility of rock. This method is described in the second section where several geomechanical parameters, such as *UCS*, K_b, K_d, J_s, J_o, *NPES*, V_b, and E_{doa}, are evaluated based on the developed method. Field data obtained from more than 100 existing

case studies and coupled with our novel approach demonstrate those geomechanical parameters that are relevant for evaluating the hydraulic erodibility of rock (Section 3). Section 4 presents a validation process of the selected parameters.

2 Description of the developed method

The proposed method for determining the relevant geomechanical parameters for evaluating the hydraulic erodibility of rock is summarized in Fig. 1. Each methodological step is described in the following subsections.

2.1 Step 1 - Establishing a dataset and an erosion-level scale

Step 1, establishing a dataset (Fig. 1), consists of collecting the data from case studies conducted on rocky dam spillways. This data includes all available information related to the geomechanical parameters that characterize rock mass, the P_a, and the observed condition of erosion. Table 1 summarizes the geomechanical parameters used by Pells (2016a) to develop the two erodibility indices of *eGSI* and *RMEI*. Some of the geomechanical parameters considered in Pells's erodibility indices are also included in Kirsten's index. Consequently, we also selected geomechanical parameters considered in Kirsten's index (Kirsten, 1982) for our dataset. For their parts, J_o and *NPES* are also included in the dataset, although they are not directly included in Kirsten's index. As K_b is an inaccurate parameter for characterizing block size (Palmstrom, 2005), we retained V_b as a parameter to be analyzed. Finally, E_{doa} is deemed synonymous to J_s for determining the effect of a rock block's shape and orientation relative to the direction of flow (Pells, 2016b; Pells et al., 2017b); we therefore included this parameter to verify its effectiveness compared to that of J_s. In summary, we retained the geomechanical parameters of M_s, K_b, K_d, J_s, J_o, *NPES*, V_b, and E_{doa}. These parameters will be analyzed for determining the relevant parameters for the evaluating the hydraulic erodibility of rock.

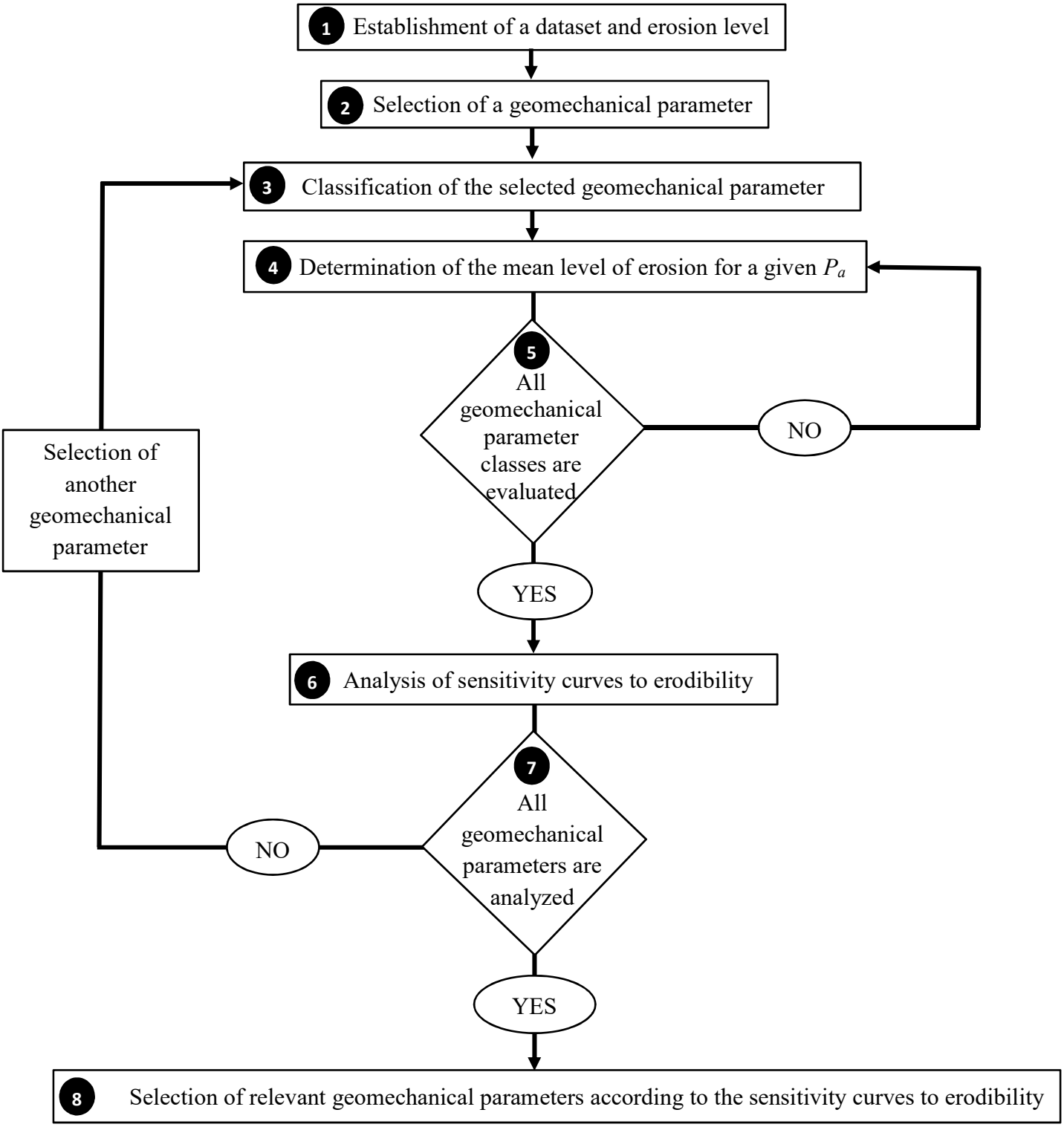

Fig. 1. Algorithm for determining the relevant geomechanical parameters for evaluating the hydraulic erodibility of rock.

Table 1. Summary of the considered geomechanical parameters.

Index	Conditions	Parameters
eGSI [1]	Strength of rock	*UCS*
	Joints condition	*RQD* Joint spacing Joint opening Roughness Infilling gouge Weathering
	Rock block condition[2]	Shape Dipping Orientation
RMEI	Joint condition	Number of joint sets Dipping Orientation Roughness *UCS* of joints Joint opening Joint spacing
	Rock block condition	Shape
	Nature of the potentially eroding surface	Protrusion of joints Opening of defects Weathering
N	Strength of rock	*UCS*
	Joint condition	*RQD* Number of joint sets Roughness Infilling gouge
	Rock block condition	Shape Dipping Orientation

1: eGSI *parameters are specified according to the RMR system.*
2: Considered as part of the E_{doa} *parameter.*

The field data collected from more than 100 case studies conducted by Pells (2016a) are presented in Appendix 1. These case studies, conducted on unlined rocky spillways of selected dams in Australia and South Africa, were selected as they provide complete data for the retained geomechanical parameters (M_s, K_b, K_d, J_s, J_o, *NPES*, V_b, and E_{doa}), the P_a, and the observed condition of erosion.

The erosion-level scale used in this study, as part of Step 1 (Fig. 1), is based on the description of the erosion condition as defined by Pells (2016a). Erosion condition is determined using the maximum depth and extension of the eroded gully (Table 2).

Table 2. Erosion condition description (Pells, 2016a).

Max. depth (m)	General extent (m^3/100 m^2)	Descriptor	Erosion level
<0.3	<10	Negligible	1
0.3–1	1–30	Minor	2
1–2	30–100	Moderate	3
2–7	100–350	Large	4
>7	>350	Extensive	5

2.2 Step 2 - Selection of a geomechanical parameter

The retained geomechanical parameters (M_s, K_b, K_d, J_s, J_o, *NPES*, V_b, and E_{doa}) are assessed individually. Therefore, Step 2 (Fig. 1) consists of selecting one geomechanical parameter from the set of retained parameters. This selected parameter is then analyzed in Steps 3–7 (Fig. 1). This process is repeated for each of the retained parameters.

2.3 Step 3 - Classification of the selected geomechanical parameter

Once a geomechanical parameter is considered for analysis (Step 2, Fig. 1), this parameter is then classified in Step 3. The objective of Step 3 is to verify the level of erosion (1 to 5; Table 2) when a given rock mass is submitted to various P_a. The classification of the geomechanical parameters relies on existing classifications from the literature or our proposed statistical classifications. In the following subsections, we describe the classifications of all retained geomechanical parameters (M_s, K_b, K_d, J_s, J_o, *NPES*, V_b, and E_{doa}).

2.3.1 *Classification of the UCS of rock*

M_s included in Kirsten's index is determined according to the *UCS* of rock, which can be estimated by performing an unconfined compressive stress test on an intact rock sample (Annandale, 2006). We use two common *UCS* scales (Tables 3 and 4).

Table 3. *UCS* classification of Jennings et al. (1973).

Class	*UCS* (MPa)	Description
1	1.7–3.3	Very soft rock
2	3.3–13.2	Soft rock
3	13.2–26.4	Hard rock
4	26.4 –106	Very hard rock
5	>106	Extremely hard rock

Table 4. *UCS* classification adopted from Bieniawski (1989, 1973).

Class	*UCS* (MPa)	Description
1	1–5	Very low strength
2	5–25	Low strength
3	25 –50	Medium strength
4	50–100	High strength
5	100–250	Very high strength
6	>250	Extremely high strength

2.3.2 *Classification of rock block size*

Classification of K_b

Block size is an extremely important parameter for evaluating rock mass behavior (Barton, 1990; ISRM, 1978). The most common indicator of block size was introduced by Cecil (1970) who combined the *RQD* index with the joint set number (J_n) to create the quotient K_b (RQD/J_n). This quotient was later adopted by Barton et al. (1974) into the Q-system and by Kirsten (1982) for his excavatability index. However, *RQD* measurements have several limitations (Grenon and Hadjigeorgiou, 2003; Palmstrom et al., 2002; Pells et al., 2017a). This parameter is included in our analyzed geomechanical parameters to verify if it can be retained as a relevant parameter for evaluating the hydraulic erodibility of rock (as previously maintained). As *RQD*

can vary from 5%–100% and J_n values vary from 1–5 (Kirsten, 1988, 1982), consequently the K_b values range from 1–100. However, there is no existing classification system for K_b. The K_b classification framework proposed in this study is based on the statistical distribution of K_b that was established through evaluating the case studies. The most representative normal distribution of K_b data is obtained based on the interval values presented in Fig. 2. Accordingly, five classes of K_b are defined (Table 5).

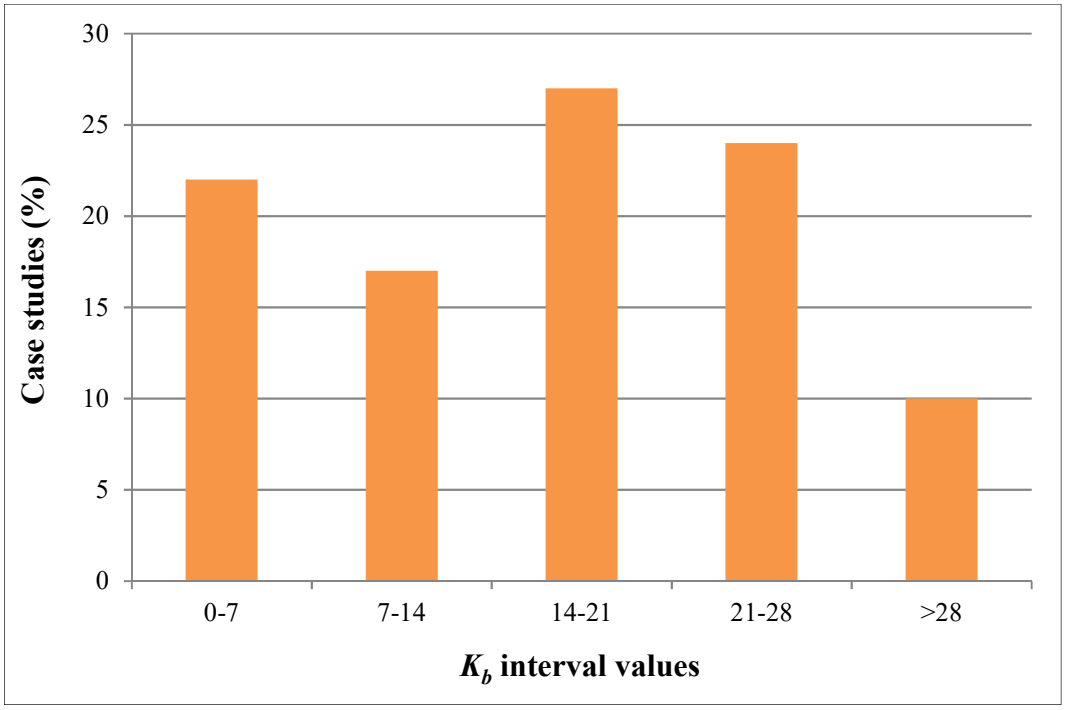

Fig. 2. The statistical distribution of K_b values from the case studies of Pells (2016a).

Table 5. Proposed K_b classification.

Class	K_b
1	0–7
2	7–14
3	14–21
4	21–28
5	>28

Classification of V_b

Palmstrom (2005) stated that using three-dimensional block volume measurements improves the characterization of block size. The block volume classification of Palmstrom (1996, 1995), presented in Table 6, is adopted for this study. Furthermore, we apply three methods (Methods 1, 2, and 3) to characterize rock block volume (Palmstrom, 2005).

Table 6. Classification of rock block volume (Palmstrom, 1995).

V_b (m^3)	Description
0.0002–0.01	Small
0.01–0.2	Moderate
0.2–10	Large
>10	Very large

Method 1

When the average joint spacing is used rather than the abundance of joint sets, the following expression is used to determine V_b (m^3):

$$V_b = Sa^3 \tag{4}$$

where Sa is the average joint spacing equal to $(S_1+S_2+S_3+S_n)/n$, where S_1, S_2, S_3…S_n is the average spacing for each of the joint sets.

Method 2

When three joint sets occur, the following expression may be used to determine V_b (m^3):

$$V_b = \frac{S_1 \cdot S_2 \cdot S_3}{Sin\ \gamma_1 \cdot Sin\ \gamma_2 \cdot Sin\ \gamma_3} \tag{5}$$

where S_1, S_2, S_3 represent the spacing of the three joint sets, and γ_1, γ_2, γ_3 represent the angles between the joint sets.

Method 3

The block volume may be determined according to:

$$V_b = \beta \cdot Jv^{-3} \quad (6)$$

where β is the block shape factor obtained through the following equation:

$$\beta = 20 + (7a_3/a_1) \quad (7)$$

where a_3 and a_1 are the shortest and longest dimensions of a block, respectively. *Jv* is defined as the number of joints intersecting a volume of 1 m³, as determined using $Jv = \lambda_1 + \lambda_2 + \lambda_3 + \lambda_n$ (where λ_1 is the joint frequency of joint set 1).

2.3.3 Classification of joint shear strength

In his index, Kirsten (1982) included K_d, as proposed by Barton et al. (1974); this quotient represents joint shear strength and is expressed as the ratio J_r/J_a, where J_r is the rating number corresponding to joint roughness, while J_a is the rating number corresponding to joint surface alteration. The J_r rating for joint conditions ranges from 0.5–4, whereas the J_a rating varies from 0.75–18 (Kirsten, 1982). Accordingly, K_d varies from 0.03–5.33; however, there is no existing classification of K_d. Based on the statistical distribution of K_d (Fig. 3), we determined four classes (Table 7). The maximum K_d value obtained from the case study data is 3.

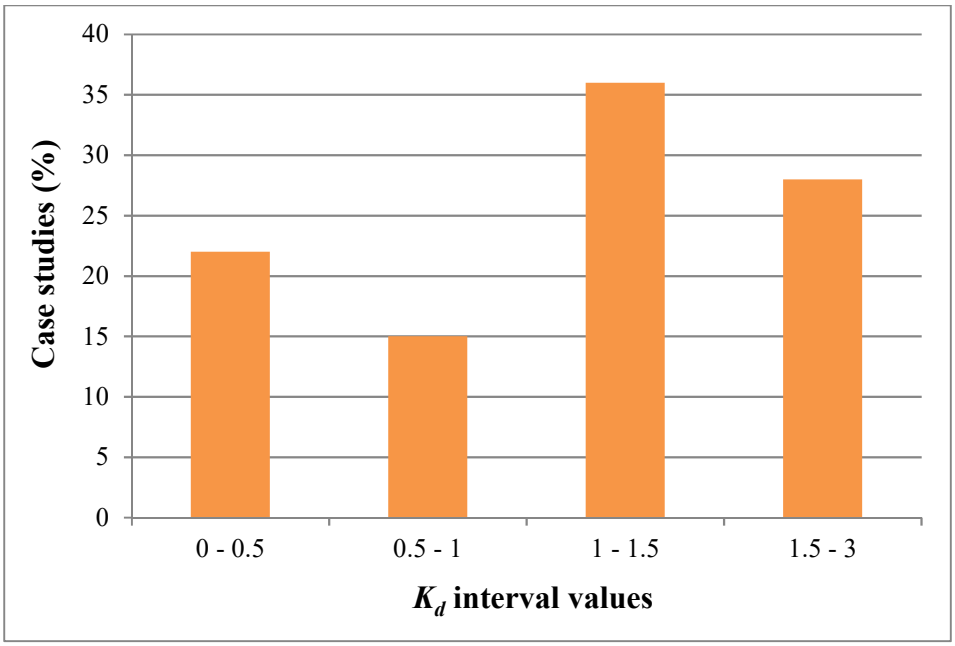

Fig. 3. The statistical distribution of K_d values from the case studies of Pells (2016a).

Table 7. Proposed K_d classification.

Class	K_d
1	0–0.5
2	0.5–1
3	1–1.5
4	1.5–3

2.3.4 Classification of a block's shape and orientation parameters

Classification of J_s

The J_s parameter included in Kirsten's index was mathematically quantified according to the effect of a block's shape and orientation relative to the direction of excavation. Its rating, as proposed by Kirsten, ranges from 0.37–1.5. As there is no existing classification of J_s, we performed a statistical distribution of the case studies data (Fig. 4). We determined five classes for J_s (Table 8). Class 4 (Table 8) is defined by the value of 1 given that there are multiple case studies having a J_s value of 1.

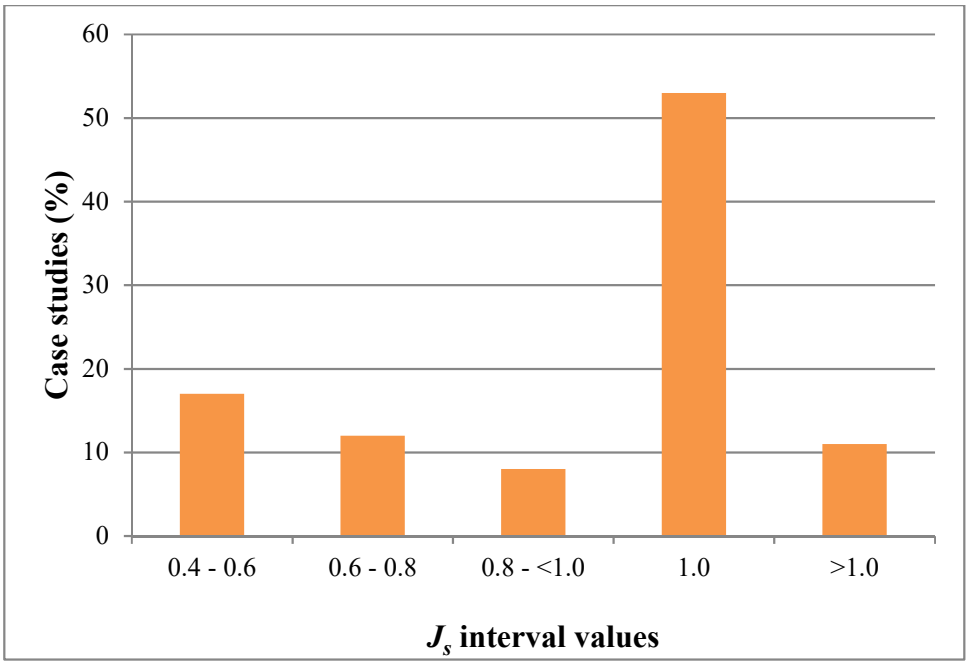

Fig. 4. The statistical distribution of J_s values obtained from the case studies of Pells (2016a).

Table 8. Proposed J_s classification.

Class	J_s	Description
1	0.4–0.6	Highly vulnerable to erosion
2	0.6–0.8	Very vulnerable to erosion
3	0.8–<1	Moderately vulnerable to erosion
4	1	Less vulnerable to erosion
5	>1	Minimally vulnerable to erosion

Classification of E_{doa}

Pells (2016a) proposed the *eGSI* index to include a new discontinuity orientation adjustment factor (E_{doa}) to represent the effect of a rock block's shape and orientation relative to the direction of flow (Eq. 2). The process of deriving values for E_{doa} was inspired from Kirsten's J_s parameter. However, values were derived purely by a thought experiment. A rock's vulnerability to significant and ongoing erosion was assessed by taking into consideration the kinematics of block removal and the nature and direction of hydraulic loading, as derived from

observation at sites and the analysis of numerous tested models (Pells, 2016a). As values of E_{doa} present the discontinuity orientation factor, they are presented as negative values, such as those included in the *RMR* system (Bieniawski, 1976).

The E_{doa} parameter is included in our list of analyzed geomechanical parameters to verify whether E_{doa} can be retained as a relevant parameter and to compare the results with those for J_s. This comparison will confirm which parameter is most representative of the effect of the block's shape and orientation. According to Pells (2016a), E_{doa} values vary from 0 to -30.

Given that there is no existing classification of E_{doa}, we assessed a statistical distribution of data from the case studies (Fig. 5), and we determined four classes for the E_{doa} parameter (Table 9). Lower values of E_{doa}, such as those included in Class 4, indicate that a rock is more vulnerable to erosion and, consequently, could be susceptible to forms of aggressive erosion.

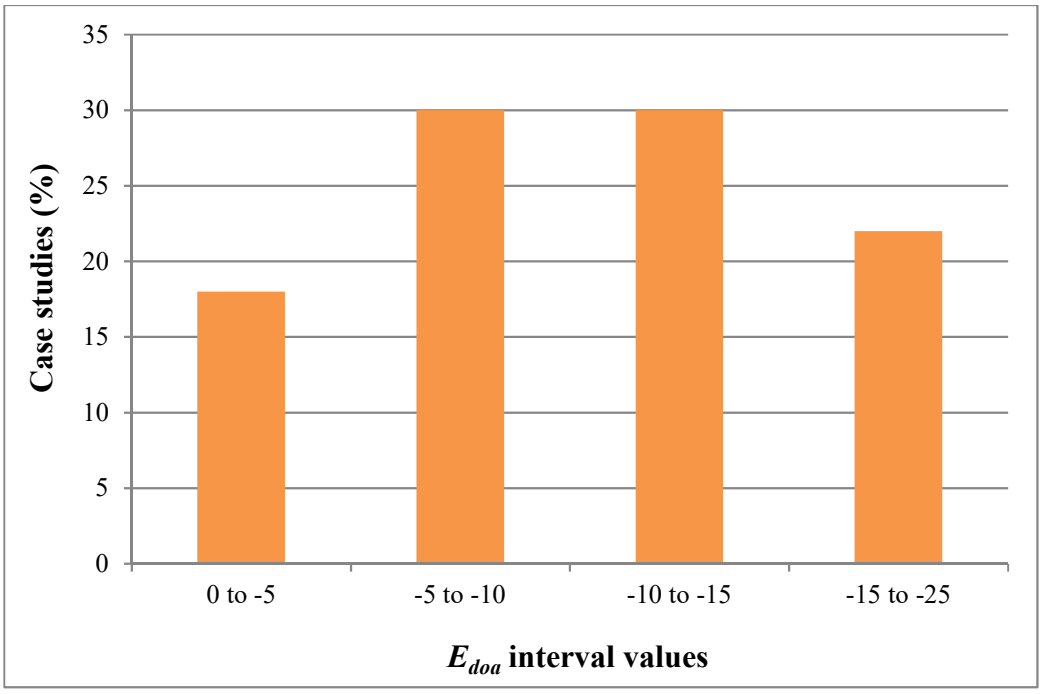

Fig. 5. The statistical distribution of E_{doa} values obtained from the case studies of Pells (2016a).

Table 9. Proposed E_{doa} classification.

Class	E_{doa}	Description
1	0 to -5	Minimally vulnerable to erosion
2	-5 to -10	Less vulnerable to erosion
3	-10 to -15	Moderately vulnerable to erosion
4	-15 to -25	Highly vulnerable to erosion

2.3.5 Classification of joint openings

Here, we adopt the joint opening classification of Bieniawski (1989), as presented in Table 10. As some case studies contain more than three joint sets, characterized by different joint opening dimensions, we use the joint opening of the joint set most sensitive to hydraulic erodibility (the joint set most oriented with the flow direction). As presented in the Appendix 1, some joint set dimensions are characterized by an interval, such as 0.1–0.5 mm. For such cases, the maximum value of the interval is retained for classification purposes.

Table 10. Joint opening classification (Bieniawski, 1989) with our proposed class.

Opening (mm)	Description	Proposed class
<0.1	Very tight	1
0.1–0.25	Tight	2
0.25–0.5	Partly open	3
0.5–2.5	Open	4
2.5–10	Widely open	5
10–100	Very widely open	6
100–1000	Extremely widely open	7
>1000	Cavernous	8

2.3.6 Classification of NPES

Our classification of *NPES* (Table 11) is adopted from the *RMEI* classification (Pells, 2016a). Spillways characterized by a Class 5 in Table 11 are the most sensitive to erosion.

Table 11. *NPES* classification (Pells, 2016a) and our proposed class.

Likelihood	Description	Proposed class
Very unlikely	Smooth water or glacier worn, no protrusions of joint 2, no opening of defects	1
Unlikely	Bedding surface with protrusions of joint 2 <1 mm, little or no opening of defects	2
Likely	Relatively small protrusions and defect openings (e.g. pre-split, or ripped and bulldozed)	3
Highly likely	Irregular surface following defects, little opening of defects (e.g. blasted rock)	4
Almost certain	Irregular surface following defects, extensive defect opening (e.g. heavily blasted rock)	5

2.4 Step 4 - Determining mean levels of erosion for given P_a categories

In Step 4, the objective is to verify erosion levels when the same rock mass class (rock mass classes are defined in Tables 3–11) is subjected to various P_a. As there are several case studies within the same geomechanical class, we determine in Step 4 the mean level of erosion for a given P_a category (Fig. 1). However, there is no existing classification of P_a. Accordingly, we performed a statistical distribution of data from the case studies (Fig. 6), and we define six P_a categories (Table 12).

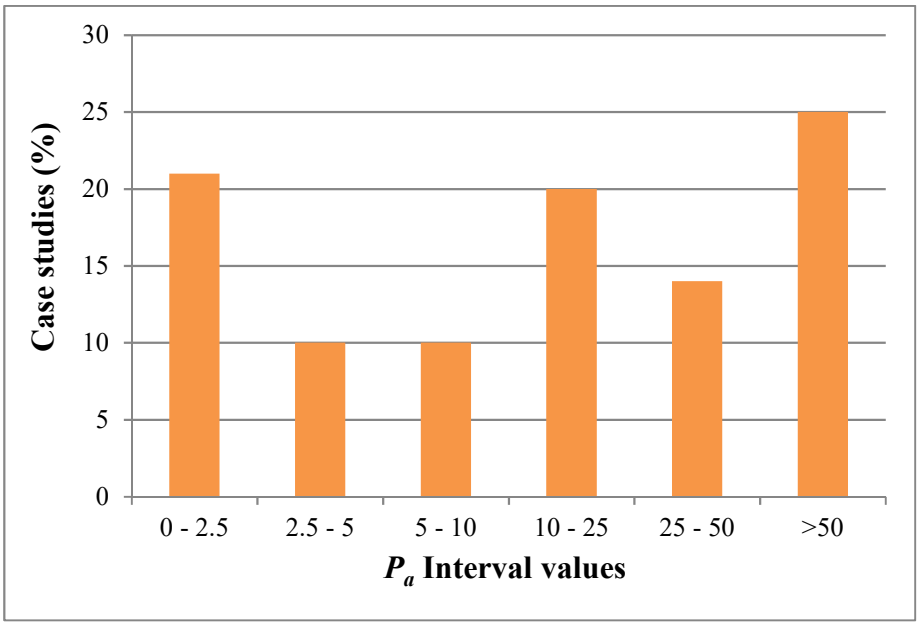

Fig. 6. Statistical distribution of P_a values from the case studies of Pells (2016a).

Table 12. Defined P_a categories.

Category	P_a (kW/m^2)
1	0–2.5
2	2.5–5
3	5–10
4	10–25
5	25–50
6	>50

The mean level of erosion for a given P_a category is calculated using Eq. (8) (Saeidi et al., 2012, 2009), where, in this study, μ_D represents the mean erosion level for a given hydraulic steam power category, and P_i is the probability of erosion level D_i, where i is ranking of the erosion level classes from 1 to 5 (Table 2). P_i is calculated according to Eq. 9, where n_i is number of case studies of erosion level D_i, and n_t is the total number of case studies, both considered for each P_a category. An example of how the mean erosion level was calculated is presented in Table 13.

$$\mu_D = \sum_{i=1}^{5} P_i \cdot D_i \tag{8}$$

$$P_i = \frac{n_i}{n_t} \tag{9}$$

Table 13. Example of calculating μ_D

Erosion class	D_i	n_i
Negligible	1	3
Minor	2	3
Moderate	3	1
Large	4	1
Extensive	5	0
	n_t	8
	μ_D	2

2.5 Step 5 – Evaluating all geomechanical parameter classes

After calculating the mean level of erosion for a P_a category (e.g. for Category 1 of Table 12; P_a = 0–2.5 kW/m^2), the identical process for calculations is then run for all P_a categories listed in Table 12. Each series of calculations for the P_a categories is run for only a single geomechanical parameter class (e.g. Class 1 of the *NPES* classification in Table 11) at a time. Accordingly, a best-fit curve representing the calculated mean level of erosion versus the average of all considered P_a categories are then plotted for this single class of geomechanical parameter. Step 5 (Fig. 1) aims to runs the identical process of calculations for each class of a single geomechanical parameter (e.g. the calculating process for classes 1 to 5 of *NPES* classification as indicated in Table 11).

2.6 Step 6 - Analysis of sensitivity curves to erodibility

A best-fit curve here is the line representing the considered points of the calculated mean level of erosion versus the average of all considered P_a categories. For each class of a single geomechanical parameter, a best-fit curve is traced. These best-curves are considered as the sensitivity curves to erodibility that could produce a synthetic value for the potential level of erosion at a given value of P_a for a specific geomechanical parameter class. These best-fit curves are used in our subsequent analyses. The main objective of Step 6 (Fig. 1) is to analyze the obtained sensitivity curves. For a geomechanical parameter, the obtained sensitivity curves to erodibility showing a logical sequence can be considered as curves associated with a relevant geomechanical parameter for evaluating the hydraulic erodibility of rock. Otherwise, it can be concluded that the analyzed geomechanical parameter cannot be considered as a relevant parameter.

2.7 Steps 7 and 8 – Analyse of all geomechanical parameters and the selection of the relevant geomechanical parameters

Step 7 consists of analyzing all retained geomechanical parameters (M_s, K_b, K_d, J_s, J_o, *NPES*, V_b, and E_{doa}) via the process described in the previous steps. Each retained parameter will have a specific sensitivity curves to erodibility. Step 8 selects the relevant geomechanical parameters for evaluating the hydraulic erodibility of rock based on the obtained sensitivity curves to erodibility. For this purpose, the sensitivity curves showing a logical sequence can be considered as curves associated with a relevant geomechanical parameter.

3 Results and discussion

3.1 Effect of the UCS of rock on erodibility

Sensitivity curves to erodibility based on the *UCS* classifications are shown in Fig. 7. For Jennings's *UCS* classification (Fig. 7a), if *UCS* controls the hydraulic erodibility process, rock masses having the highest *UCS*, such as the extremely hard rock class in Table 3 (>106 MPa), should produce the least sensitive erodibility curves, whereas a lower *UCS*, such as the hard rock class in Table 3 (13.2–26.4 MPa), should generate the most sensitive erodibility curve. As expected, the extremely hard rock class (>106 MPa) produces the least sensitive curve; however, the very hard rock class (26.4–106 MPa) has the most sensitive erodibility curve, rather than the hard rock class (Fig. 7a) that has a lower *UCS* interval (13.2–26.4 MPa). Given this inversion of the generated sensitivity curves to erodibility for hard and very hard rock classes, it is difficult to justify using *UCS* in assessing the hydraulic erodibility process.

Sensitivity curves to erodibility based on Bieniawski's *UCS* classification (Table 4) are shown in Fig. 7b. Rock masses characterized by the highest *UCS* values, such as the extremely strength class in (>250 MPa, Table 4), should produce the least sensitive curve to erodibility,

whereas rock masses having the lowest *UCS* values, such as the low-strength class (5–25 MPa, Table 4), should generate the most sensitive curve. However, we observe (Fig. 7b) that the most sensitive erodibility curve is obtained for the high strength rock class (50–100 MPa), whereas the least sensitive curve to erodibility is for the very high strength rock class (100–250 MPa). Surprisingly, the sensitivity curve to erodibility for the extremely high strength class (>250 MPa) is the second-most sensitive curve. Furthermore, sensitivity curves to erodibility of the low-strength class and medium strength class are misplaced from the expected pattern (Fig. 7b). These two sensitivity curves to erodibility should be placed at the top as the more sensitive erodibility curves according to their *UCS* of 5–25 MPa and 25–50 MPa, respectively, rather than being placed as moderately sensitive curves. As *UCS* sensitivity curves to erodibility, according to Bieniawski's *UCS* classification, show a random sequence (and a similar pattern is observed using Jennings's *UCS*), *UCS* cannot be considered as a relevant parameter for evaluating the hydraulic erodibility of rock.

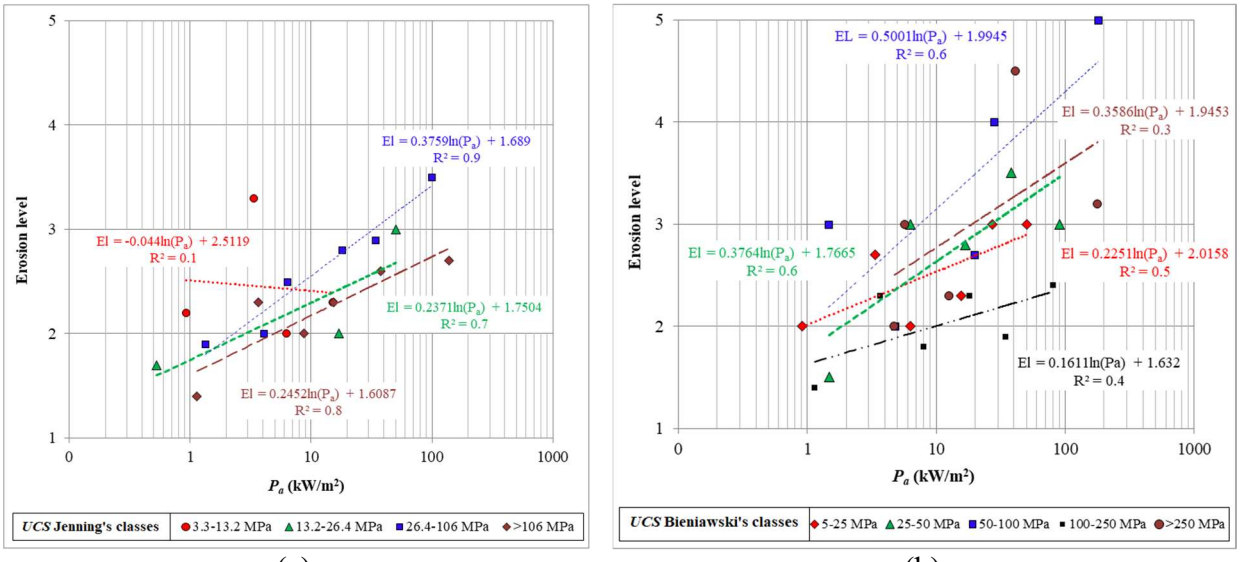

(a) (b)

Fig. 7. Sensitivity curves to erodibility based on *UCS*: a) Jenning's *UCS* classification; b) Bieniawski's *UCS* classification. Each best-fit line and its equation correspond to the same symbol data points, which are also represented by the same color.

3.2 Effect of rock block size on erodibility

Rock block volume V_b was calculated using the three described methods (Section 2.2.2). Sensitivity curves to erodibility according to rock block size (K_b and V_b) are shown in Fig. 8. Sensitivity curves to erodibility based on K_b show that a rock mass characterized by a K_b of Class 1 (K_b = 0–7) is, as expected, the most sensitive to erodibility (Fig. 8a). However, this curve is intersected by the curve representing Class 2 (K_b = 7–14) when P_a = 60 kW/m^2. Accordingly, Class 2 becomes subsequently more sensitive than Class 1 as P_a increases. On the other hand, the sensitivity curves to erodibility for classes 3 and 5 decrease as P_a increases. This is not logical as an increased P_a should beget an increase in the amount of erosion. Also, the sensitivity curve to erodibility representing Class 2 (K_b = 7–14) is more sensitive than the Class 4 sensitivity curve to erodibility (K_b = 21–18); however, this pattern is only observed when P_a is >4 kW/m^2. Below this threshold, Class 4 is more sensitive to erodibility than Class 2, rendering this behavior invalid. Given these patterns, K_b cannot be selected as a relevant parameter for evaluating the hydraulic erodibility of rock.

Sensitivity curves to erodibility based on V_b, when V_b is calculated according to Method 1, show that for moderate, large, and very large classes, very large volumes (>10 m^2) are the least sensitive to erodibility, and sensitivity is subsequently more important as V_b decreases (Fig. 8b). However, this is only noted when P_a is >6 kW/m^2. Method 1 thus provides a good evaluation for a large range of P_a values; however, at values <6 kW/m^2, Method 1 produces invalid results. Similar patterns are observed when V_b is calculated via Method 2 (Fig. 8c) and Method 3 (Fig. 8d). Methods 2 and 3 provide a good evaluation, although only when P_a values are >10 kW/m^2 and >1 kW/m^2, respectively.

Overall, use of the three-dimensional block volume measurement, rather than the K_b parameter, provides a better characterization of the rock block size. Palmstrom (2005) argues that their method (Palmstrom 1995, 1996), based on volumetric joint count (Method 3), provides the best characterization of the block volume. We also select this method as it provides a good evaluation for much of the range for P_a relative to methods 1 and 2.

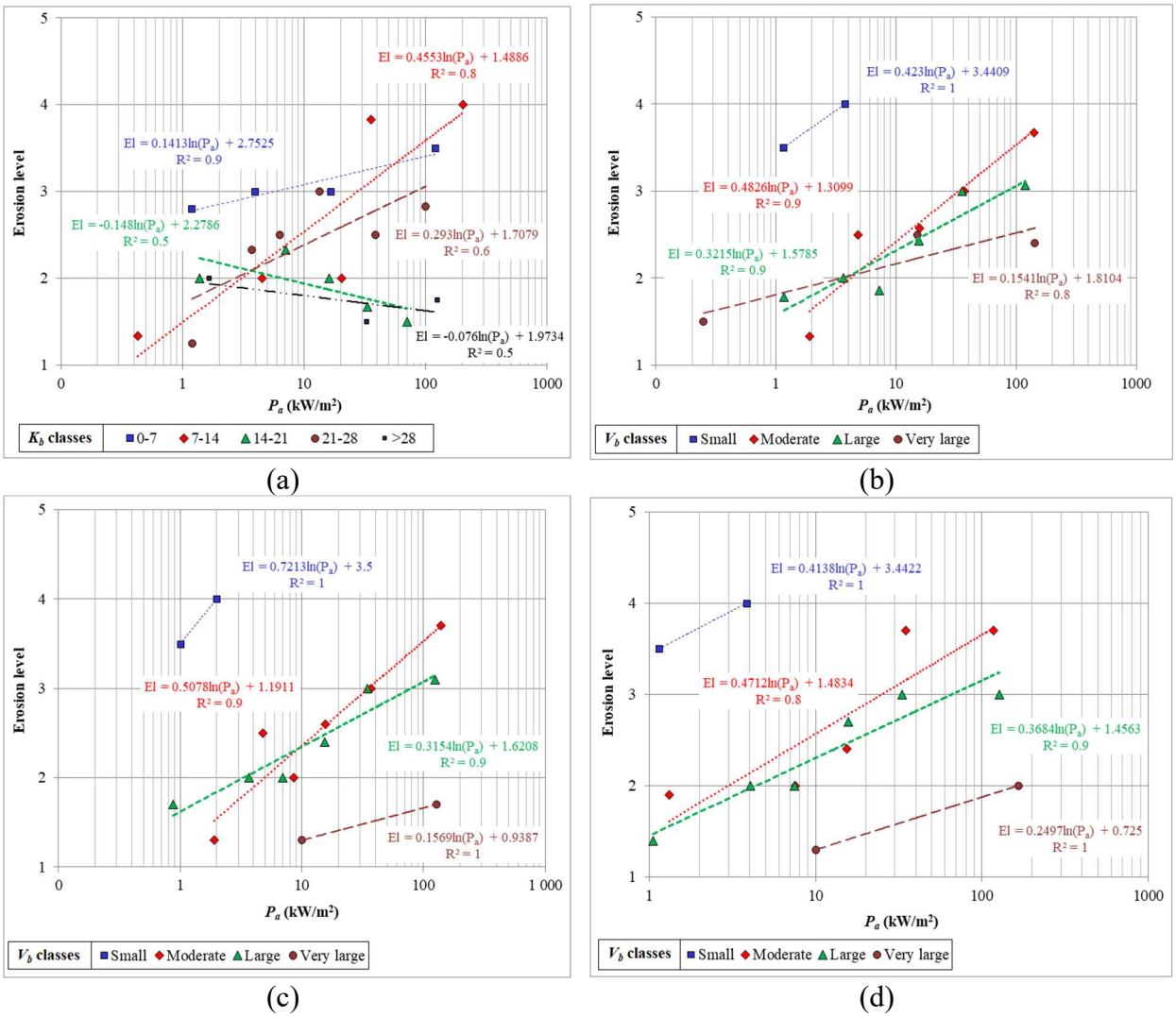

Fig. 8. Sensitivity curves to erodibility based on rock block size: a) K_b classification; b) V_b classification (V_b calculated according to Method 1); c) V_b classification (V_b calculated according to Method 2); d) V_b classification (V_b calculated according to Method 3). Each best-fit line and its equation correspond to the same symbol data points, which are also represented by the same color.

3.3 Effect of joint shear strength on erodibility

As K_d indicates joint shear strength, rock mass characterized by a K_d of Class 1 (K_d = 0–0.5), as described in Table 7, should be more sensitive to erodibility than other rock masses characterized, for example, by a K_d of Class 4 (K_d = 1.5–3). Sensitivity curves to erodibility based on the K_d classification (Table 7) follow the K_d categories perfectly (Fig. 9). Case studies of Class 4 (K_d = 1.5–3) are the least sensitive to erodibility, and sensitivity is subsequently greater as K_d decreases. With a P_a value of 10 kW/m^2, for example, a Class 4 rock mass (K_d = 1.5–3) would have negligible to minor erosion, whereas a Class 1 rock mass (K_d = 0–0.5) would have moderate erosion. As K_d sensitivity curves to erodibility show a logical sequence having a proportional relationship between joint shear strength and the level of erosion (when joint shear strength decreases, erosion is greater), K_d can be retained as a relevant parameter for evaluating the hydraulic erodibility of rock.

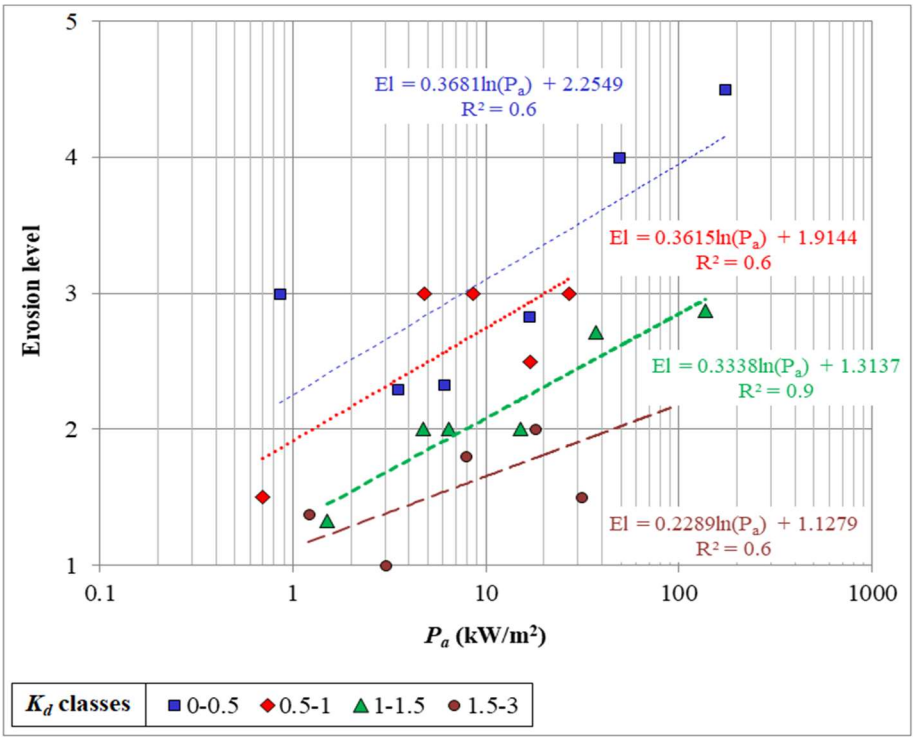

Fig. 9. Sensitivity curves to erodibility based on K_d classification. Each best-fit line and its equation correspond to the same symbol data points, which are also represented by the same color.

3.4 Effect of a block's shape and orientation on erodibility

Sensitivity curves to erodibility based on J_s classification (Table 8) show that Class 1 (J_s = 0.4–0.6) decreases as P_a increases (Fig. 10a). This is considered as a random pattern as increased P_a should beget increased levels of erosion. Also, multiple intersecting points are noted between the sensitivity curves to erodibility; for example, the Class 2 sensitivity curve (J_s = 0.6–0.8) intersects with the Class 4 curve (J_s = 1) at P_a = 10 kW/m^2. This confusing observation is also noted for classes 3 and 5 at a P_a of 50 kW/m^2. Random patterns of the J_s sensitivity curves complicate the use of J_s as a relevant parameter for evaluating the hydraulic erodibility of rock.

The E_{doa} parameter is proposed as an indicator of the effect of a rock block's shape and its orientation relative to the direction of flow. The lowest values of E_{doa}, such as those included of Class 4 (E_{doa} = -15 to -25), indicate that the rock mass would be greatly susceptible to erosion. Based on the sensitivity curves to erodibility in Fig. 10b, Class 1 rock masses (E_{doa} = 0 to -5) are the least sensitive, and sensitivity increases as E_{doa} decreases. At a P_a of 100 kW/m^2, for example, a Class 1 rock mass (E_{doa} = 0 to -5) would have undergone minor levels of erosion, whereas a Class 4 rock mass (E_{doa} = -15 to -25) would have experienced marked erosion. As E_{doa} sensitivity curves to erodibility show a logical sequence having a proportional relationship between E_{doa} and the level of erosion (as E_{doa} decreases, erosion increases), E_{doa} is retained as a relevant parameter for evaluating the hydraulic erodibility of rock.

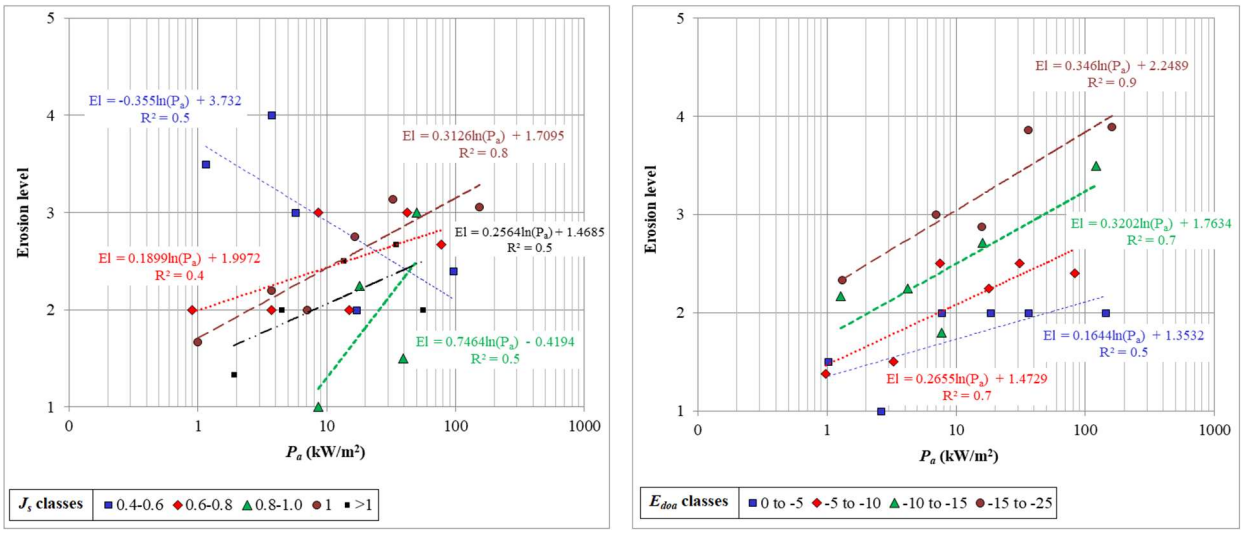

(a) (b)

Fig. 10. Sensitivity curves to erodibility based on a block's shape and orientation relative to the direction of flow: a) J_s classification; b) E_{doa} classification. Each best-fit line and its equation correspond to the same symbol data points, which are also represented by the same color.

3.5 Effect of joint opening on erodibility

Sensitivity curves to erodibility based on J_o classification (Table 10) are aligned according to J_o (Fig. 11). Case studies having a tight joint opening (J_o <0.25 mm) are the least sensitive to erosion, and sensitivity to erodibility increases as J_o increases. At a P_a of 100 kW/m^2, for example, a rock mass having tight joint openings (<0.25 mm) would experience minor erosion, whereas a rock mass having widely open joints (2.5–10 mm) would experience marked erosion. As J_o sensitivity curves to erodibility show a logical pattern and have a proportional relationship between joint opening and the level of erosion (as J_o increases, erosion is greater), J_o is considered as a relevant parameters for evaluating the hydraulic erodibility of rock.

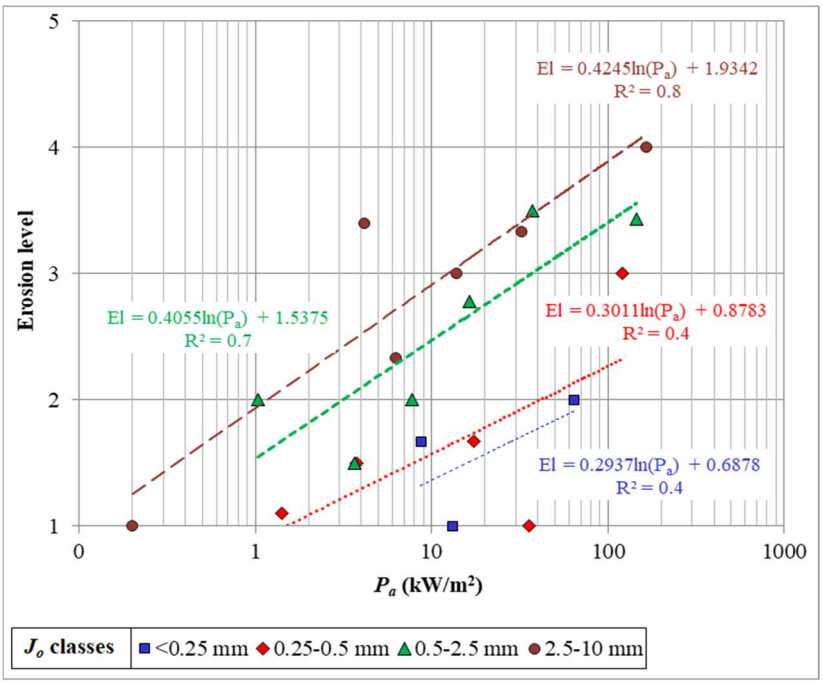

Fig. 11. Sensitivity curves to erodibility based on J_o classification. Each best-fit line and its equation correspond to the same symbol data points, which are also represented by the same color.

3.6 Effect of NPES on erodibility

Sensitivity curves to erodibility based on NPES classification show that this parameter has a proportional relationship to erosion (Fig. 12). Class 2 rock mass (Class 2 includes a flowing surface with an unlikely potential for erosion, Table 11) is the least sensitive to erosion, while Class 5 rock mass (Class 5 includes a flowing surface having an almost certain potential for erosion, Table 11) is most sensitive. Transmitted flow energy, in the case of an irregular flowing surface, can be greater than that for a smooth flowing surface (Annandale, 2006). Other sensitivity curves to erodibility associated with classes 3, 4, and 5 are also plotted (Fig. 12) and show a similar relationship to P_a. As *NPES* sensitivity curves to erodibility show a logical relationship to P_a, *NPES* is retained as a relevant parameter for evaluating the hydraulic erodibility of rock.

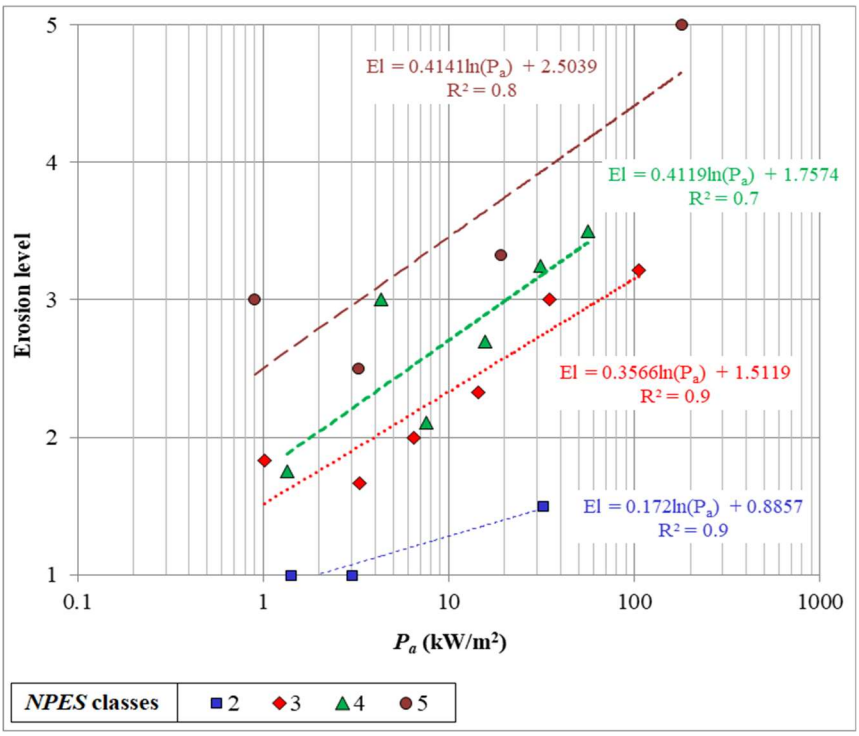

Fig. 12. Sensitivity curves to erodibility based on *NPES* classification. Each best-fit line and its equation correspond to the same symbol data points, which are also represented by the same color.

From our analysis of the sensitivity curves to erodibility, five parameters (J_o, K_d, V_b, E_{doa}, and *NPES*) are retained as relevant parameters for evaluating the hydraulic erodibility of rock (Step 8 - Fig. 1). *UCS*, K_b, and *Js* present some random or illogical patterns related to the erosion condition and, consequently, are not considered further. The selected parameters can be used for developing new erodibility index for evaluating the hydraulic erodibility of rock.

3.7 Validation of developed methodology

We can determine the individual effect of each geomechanical parameter. However, the selected geomechanical parameters (J_o, V_b, K_d, E_{doa}, and *NPES*) could interact via-à-vis their effect on the level of erosion. Accordingly, it is important to validate whether the obtained

sensitivity curves to erodibility for a given parameter provide a reliable prediction of erosion level when all selected parameters are considered. To validate the J_o sensitivity curves to erodibility for this purpose, we selected from the existing case studies those cases having the same geomechanical parameter class for V_b, K_d, E_{doa}, and *NPES*, while the parameter J_o is omitted from this selection. If this subset of case studies having identical geomechanical parameter classes (except for J_o) are characterized by differing levels of erosion, then the differences in the degree of erosion are influenced by J_o. Erosion level and P_a associated with this subset of case studies (where V_b, K_d, E_{doa}, and *NPES* values are similar) are plotted on J_o sensitivity curves to erodibility (Fig. 11) to verify whether the observed erosion agrees with the J_o sensitivity curves to erodibility. This approach is then repeated for each of the selected parameters (each parameter is isolated from the other four parameters), and the obtained results are shown in Fig. 13. For each parameter validation, ten case studies were used. The exception was the validation process of V_b where nine case studies were used (Fig. 13). In Fig. 13, the colored dashed lines present the sensitivity curves to erodibility for the selected parameters, as explained in the previous section. The individual symbols are the observed case studies data that are plotted on Fig. 13a to 13e (e.g. for the validation of the *NPES* parameter presented in Fig. 13e, the colored dashed lines are the sensitivity curves to erodibility developed for this parameter. The associated symbols are the data from the observed case studies, and their color corresponds to their class).

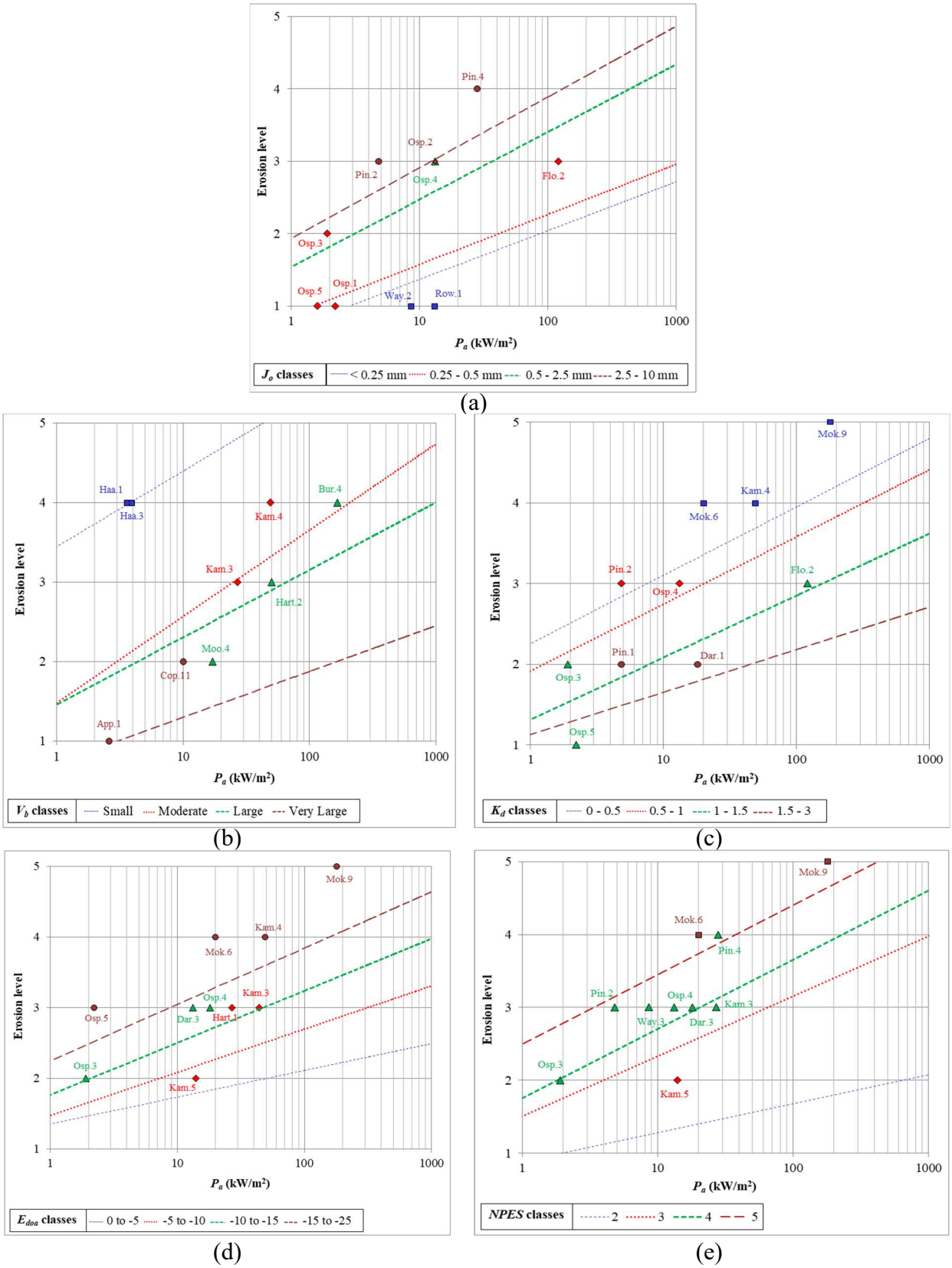

Fig. 13. Validation based on a) J_o sensitivity curves; b) V_b sensitivity curves; c) K_d sensitivity curves; d) E_{doa} sensitivity curves; and e) *NPES* sensitivity curves.

Some case studies agree perfectly with the developed sensitivity curves to erodibility. The case studies in agreement with the sensitivity curves include the case study Osp.2 introduced to validate J_o sensitivity curves (Fig. 13a), Haa.1, Haa.3, Kam.3, and Opp.1 used to validate the V_b curves (Fig. 13b), Flo.2 plotted on the K_d sensitivity curves (Fig. 13c), Osp.3 used to validate the E_{oda} curves (Fig. 13d), and Dar.3 and Osp.3 plotted on the *NPES* sensitivity curves to erodibility (Fig. 13e). Nonetheless, certain case studies do not agree perfectly with the developed sensitivity curves to erodibility (Fig. 13). To determine the efficiency of the obtained results, we use the root mean square error (RMSE). In geosciences, RMSE is often used to assess modeling quality both in terms of accuracy and precision (Boumaiza et al., 2019; Gokceoglu and Zorlu, 2004; Wise, 2000; Zimmerman et al., 1999). In this study, as shown in Eq. (10), RMSE corresponds to the mean of differences between the theoretical level of erosion ($El_{Supposed}$) as determined via the developed sensitivity curves to erodibility, and the actual level of erosion (El_{Real}) observed in the field. The calculated RMSE (named Real RMSE) indicates the produced error according to the obtained result.

$$RMSE = \left(\frac{1}{n}\sum_{i=1}^{n}\left(El_{Supposed} - El_{Real}\right)^2\right)^{1/2} \quad (10)$$

To determine the maximum possible error (named Max RMSE), the actual erosion level (El_{Real}) is replaced, in a second step, by the level of erosion that produces a Max RMSE. The maximum level of erosion that could be eventually produced, according to Table 2, represents the extensive erosion corresponding to a value of 5. An example of the calculations is presented in Table 14.

Table 14. RMSE calculating process according to J_o sensitivity curves to erodibility.

ID	Theoretical level of erosion [1]	Actual level of erosion	Max. level of erosion
Pin.4	3	4	5
Osp.2	3	3	5
Pin.2	3	3	5
Osp.4	3	3	5
Flo.2	2	3	5
Osp.3	1	2	5
Osp.5	1	1	5
Osp.1	1	1	5
Way.2	1	1	5
Row.1	1	1	5
	Real RMSE	**0.49**	
		Max RMSE	**3.13**

1: Rounded values determined from sensitivity curves shown in Fig. 13a.

The ratio of real RMSE to max RMSE indicates the magnitude associated to the actual produced error compared to the maximum possible produced error. Table 15 presents Real and Max RMSE values, calculated based on sensitivity curves to erodibility for each of the selected parameters presented in Fig. 13, and the determined ratio (%). Real RMSE is always lower than Max RMSE, where the determined ratio of Real RMSE to Max RMSE varies from 16% (for J_o sensitivity curves to erodibility) to 42% (for E_{doa} and *NPES* sensitivity curves to erodibility) (Table 15). Consequently, the real produced error according to our method can be considered acceptable compared to the maximum produced error, and this verification confirms the efficiency of the proposed methodology.

Table 15. Calculated RMSE and the determined ratio.

Parameter	J_o	V_b	K_d	E_{doa}	*NPES*
Real RMSE	0.49	1.12	1.07	1.33	1.33
Max RMSE	3.13	3.13	3.18	3.18	3.18
Ratio (%)	16	36	34	42	42

4 Conclusion

Our method for determining relevant rock mass parameters in the evaluation of the hydraulic erodibility of rock is derived from case studies of erosion in unlined rocky spillways of selected dams in Australia and South Africa. As the hydraulic erodibility of rock is a physical process controlled by a group of rock mass geomechanical parameters, several geomechanical parameters of rock mass (*UCS*, K_b, K_d, J_s, J_o, *NPES*, V_b, and E_{doa}) were analyzed to determine those parameters that are relevant for evaluating the hydraulic erodibility of rock. We find that the *UCS* of rock does not have a significant effect on hydraulic erodibility. The K_b parameter, defined to represent rock block size in the context of hydraulic erodibility, can be improved by replacing it with the V_b parameter. Given the importance of a block's orientation and shape relative to the direction of flow in the erodibility process, the E_{doa} parameter is determined as a more relevant parameter than J_s. For their part, parameters associated with joint conditions (K_d and J_o) and *NPES* parameter are retained as relevant geomechanical parameters for evaluating the hydraulic erodibility of rock.

Kirsten's index includes some parameters (*UCS*, K_b and J_s) that our method deemed to be non-relevant parameters for evaluating the hydraulic erodibility of rock, and it is concluded that the use of the three-dimensional block volume measurement (V_b), rather than the K_b parameter, could improve the characterization of rock block size. Furthermore, the J_o and V_b parameters are determined as relevant parameters for evaluating the hydraulic erodibility of rock. However, *eGSI* index does not consider them when *GSI* is determined from Marinos & Hoek (2000) chart. Finally, it concluded that determining the relevant geomechanical parameters for evaluating the hydraulic erodibility of rock, as determined in this study, could be very useful

key-step to develop a new hydraulic erodibility index, one that could be used to provide a more accurate assessment of the hydraulic erodibility of rock.

Conflict of interest

The authors confirm that there are no known conflicts of interest associated with this publication, and there has been no significant financial support for this work that could have influenced its outcome.

Acknowledgments

The authors would like to thank the organizations that have funded this project: Natural Sciences and Engineering Research Council of Canada (Grant No. 498020-16), Hydro-Quebec (NC-525700), and the Mitacs Accelerate program (Grant Ref. IT10008).

References

Annandale GW. Scour Technology, Mechanics and Engineering in Practice. McGraw-Hill, New York; 2006.

Annandale GW. Erodibility. Journal of Hydraulic Research 1995;33:471–94.

Annandale GW, Kirsten HAD. On the erodibility of rock and other earth materials. Hydraulic Engineering 1994;1:68–72.

Annandale GW, Ruff JF, Wittler RJ, T.M. L. Prototype validation of erodibility index for scour in fractured rock media. Proceedings of the International Water Resources Engineering Conference, Memphis, Tennessee, American Society, 1998, p. 1096–101.

Barton N. Scale effects or sampling bias. Proceeding of International Workshop Scale Effects in Rock Masses, Balkema Publication, Rotterdam, 1990, p. 31–55.

Barton N, Lien R, Lunde J. Engineering classification of rock masses for the design of tunnel support. Rock Mechanics 1974;6:189–236.

Bieniawski ZT. Engineering rock mass classifications : a complete manual for engineers and geologists in mining, civil, and petroleum engineering 1989:251.

Bieniawski ZT. Rock mass classification in rock engineering. In Exploration for rock

engineering, procedures of the symposium. ZT Bieniawski, Cape Town: Balkema 1976:97–106.

Bieniawski ZT. Engineering Classification of Jointed Rock Masses. The Civil Engineer in South Africa 1973;15:343–53.

Boumaiza L, Saeidi A, Quirion M. Determining relative block structure rating for rock erodibility evaluation in the case of non-orthogonal joint sets. Journal of Rock Mechanics and Geotechnical Engineering 2019;11:72–87.

Boumaiza L, Saeidi A, Quirion M. Evaluation of the impact of the geomechanical factors of the Kirsten's index on the shifting-up of rock mass erodibility class. Proceeding of The 70th Canadian Geotechnical Conference and the 12th Joint CGS/IAH-CNC Groundwater Conference, Ottawa, Ontario, Canada, 2017, p. 8.

Castillo LG, Carrillo JM. Scour, velocities and pressures evaluations produced by spillway and outlets of dam. Water 2016;8:1–21.

Cecil OS. Correlations of rock bolt-shotcrete support and rock quality parameters in Scandinavian tunnels. Ph.D Thesis., Urbana, University of Illinois, (cited in Barton et al., 1974); 1970.

Doog N. Die hidrouliese erodeerbaarheid van rotmassas in onbelynde oorlope met spesiale verwysing na die rol van naatvulmateriaal. Master thesis in Afrikaans language, University of Pretoria, South Africa; 1993.

Gokceoglu C, Zorlu K. A fuzzy model to predict the uniaxial compressive strength and the modulus of elasticity of a problematic rock. Engineering Applications of Artificial Intelligence 2004;17:61–72.

Goodman RE. Engineering geology-Rock in engineering construction. John Wiley & Sons, New York; 1993.

Grenon M, Hadjigeorgiou J. Evaluating discontinuity network characterization tools through mining case studies. Soil Rock America 2003;1:137–42.

Hadjigeorgiou J, Poulin R. Assessment of ease of excavation of surface mines. Journal of Terramechanics 1998;35:137–53.

Hahn WF, Drain MA. Investigation of the erosion potential of kingsley dam emergency spillway. Proceeding of the joint Annual Meeting and Conference of AIPG, AGWT, and the Florida Section of AIPG, Orlando, Florida, USA., 2010, p. 1–10.

Hoek E, Kaiser PK, Bawden WF. Support of underground excavations in hard rock. A.A. Balkema/Rotterdam/Brookfield.; 1995.

ISRM (International Society for Rock Mechanics). Suggested methods for the quantitative description of discontinuities in rock masses. International Journal of Rock Mechanics and

Mining Sciences & Geomechanics Abstracts 1978;15:319–68.

Jennings JE., Brink ABA, Williams AAB. Revised guide to soil profiling for civil engineering purposes in South Africa. Civil Engineering in South Africa 1973;15:3–12.

Kirkaldie L. Rock classification systems for engineering purposes. American Society for Testing and Materials, ASTM STP-984, Philadephia, PA 1988.

Kirsten HAD. Case histories of groundmass characterization for excavatability. Rock Classification Systems for Enginering Purposes American Society for Testing and Materials, STP 984 1988:102–20.

Kirsten HAD. A classification system for excavation in natural materials. The Civil Engineer in South Africa 1982;24:292–308.

Kirsten HAD, Moore JS, Kirsten LH, Temple DM. Erodibility criterion for auxiliary spillways of dams. Journal of Sediment Research 2000;15:93–107.

Kuroiwa J, Ruff JF, Wittler RJ, Annandale GW. Prototype Scour Experiment in Fractured rock media. Proceedings of International Water Resources Engineering Conference and Mini-Symposia, ASCE, Memphis, TN., 1998.

Laugier F, Leturcq T, Blancer B. Stabilité des barrages en crue : Méthodes d'estimation du risque d'érodabilité aval des fondations soumises à déversement par-dessus la crête. Proceeding de la Fondation des barrages. Chambery, France, 2015, p. 125–36.

Marinos P, Hoek E. GSI: A geologically friendly tool for rock mass strength estimation. Proc. GeoEng2000 Conference, 2000, p. 1422–42.

Moore JS. The characterization of rock for hydraulic erodibility. SCS Technical Release - 78, Northeast National Technical Center, Chester. PA. (Cited in Van Schalkway et al., 1994); 1991.

Moore JS, Kirsten HAD. Discussion – Critique of the rock material classification procedure. Rock classification systems for engineering purposes. American Society for Testing and Materials, STP-984, L. Kirkaldie Ed, Philadephia, 1988, p. 55–8.

Moore JS, Temple DM, Kirsten HAD. Headcut advance threshold in earth spillways. Bulletin of the Association of Engineering Geologists 1994;31:277–80.

Mörén L, Sjöberg J. Rock erosion in spillway channels – A case study of the Ligga spillway. Proceedings of 11th Congress of the International Society for Rock Mechanics, Lisbon, Portugal, 2007, p. 87–90.

Palmstrom A. Measurements of and correlations between block size and rock quality designation (RQD). Tunnelling and Underground Space Technology 2005;20:362–77.

Palmstrom A. Characterizing rock masses by the RMi for Use in Practical Rock Engineering.

Part 1: The development of the Rock Mass index (RMi). Tunnelling and Underground Space Technology 1996;ll:175–88.

Palmstrom A. RMi--a rock mass characterization system for rock engineering purposes. Ph.D. thesis, University of Oslo, Norway, 1995.

Palmstrom A, Blindheim OT, Broch E. The Q-system – possibilities and limitations (in Norwegian). Norwegian National Conference on Tunnelling. Norwegian Tunnelling Association, Oslo, Norway, 2002, p. 41.1-41.43.

Palmstrom A, Broch E. Use and misuse of rock mass classification systems with particular reference to the Q-system. Tunnelling and Underground Space Technology 2006;21:575–93.

Pells SE. Erosion of rock in spillways. Ph.D Thesis, University of New South Wales, Australia; 2016a.

Pells SE. Assessment and surveillance of erosion risk in unlined spillways. Proceeding of International symposium on Appropriate technology to ensure proper development, operation and maintenance of dams in developing countries", Johannesburg, South Africa, 2016b, p. 269–78.

Pells SE, Bieniawski ZT, Hencher S, Pells PJN. RQD: Time to Rest in Peace. Canadian Geotechnical Journal 2017a;54:825–34.

Pells SE, Douglas K, Pells PJN, Fell R, Peirson WL. Rock mass erodibility. Technical Note: Journal of Hydraulic Engineering 2017b;43:1–8.

Pells SE, Pells PJN, Peirson WL, Douglas K, Fell R. Erosion of unlined spillways In Rock - does a "scour threshold" exist? Proceeding of Australian National Committee on Large Dams . Brisbane, Queensland, Australie, 2015, p. 1–9.

Pitsiou S. The effect of discontinuites of the erodibility of rock in unlined spillways of dams. Master's Thesis, University of Pretoria, South Africa; 1990.

Rock AJ. A semi-empirical assessment of plung pool scour: Two-dimensional application of Annandale's Erodibility Method on four dams in British Colombia, Canada. Master's Thesis, University of British Columbia. Vancouver, British Columbia, Canada; 2015.

Rouse H, Ince S. History of hydraulics. Iowa Institute of Hydraulic Research, State University of Iowa; 1957.

Saeidi A, Deck O, Verdel T. Development of building vulnerability functions in subsidence regions from analytical methods. Géotechnique 2012;62:107–20.

Saeidi A, Deck O, Verdel T. Development of building vulnerability functions in subsidence regions from empirical methods. Engineering Structures 2009;31:2275–86.

Scoble MJ, Hadjigeorgiou J, Nenonen L. Development of an excavating equipment selection

expert system, based on geotechnical considerations. Proccedings of the 40th Canadian Geotechnical Conference, Regina, 1987, p. 67–78.

Van-Schalkwyk A. Watenavorsingskommissie: Verslag oor loodsondersoek: Die erodeebaarheid van verskillende rotsformasies in onbeklede damoorlope,. Unpublished report, University of Pretoria, South Africa (Cited in Van Schalkwayk et al., 1994); 1989.

Van-Schalkwyk A, Jordaan J, Dooge N. Erosion of rock in unlined spillways. Proceeding of International Commission on Large Dams, Paris, 71 (37), 1994, p. 555–71.

Weaver JM. Geological factors significant in the assessment of rippability. The Civil Engineer in South Africa 1975;17:313–6.

Wise S. Assessing the quality for hydrological applications of digital elevation models derived from contours. Hydrological Processes 2000;14:1909–29.

Wittler RJ, Annandale GW, Ruff JF, Abt SR. Prototype validation of erodibility index for scour in granular media. International Water Resources Engineering Conference, Memphis, Tennessee, American Society of Civil Engineers., 1998, p. 1090–5.

Zimmerman D, Pavlik C, Ruggles A, Armstrong MP. An experimental comparison of ordinary and universal kriging and inverse distance weighting. Mathematical Geology 1999;31:375–90.

Appendix 1. Summary of the data used in this study

ID	UCS (MPa)	K_b -	K_d -	J_o (mm)	J_s -	E_{doa} -	NPES -	Erosion condition	P_a (kW/m^2)	ID	UCS (MPa)	K_b -	K_d -	J_o (mm)	J_s -	E_{doa} -	NPES -	Erosion condition	P_a (kW/m^2)
Ant. 1	35	17.70	2.00	<1	0.7	-8	4	Minor	1.7	Haa.4	13	5.90	0.33	2.5-10	0.48	-15	-	Large	2
Ant. 2	35	11.74	2.00	0.1-0.5	0.7	-8	3	Negligible	0.8	Har.1	140	25.07	0.50	<1	1	-5	4	Minor	0.6
Ant. 3	35	17.70	2.00	1-2	0.7	-8	4	Minor	0.7	Har.2	140	32.61	0.50	1-2	1	-5	4	Minor	1
Ant. 4	35	27.17	2.00	2-5	1	-18	2	Moderate	6.3	Har.3	140	30.52	1.00	<1	1	-5	4	Minor	1
App.1	50	18.32	0.38	0.5-2.5	0.6	-5	3	Negligible	2.6	Har.4	140	32.61	1.00	-	1.1	-10	4	Minor	56
App.2	50	18.32	0.38	0.5-2.5	0.6	-8	3	Minor	15	Hart.1	180	20.96	1.25	0.1-0.5	0.8	-5	4	Negligible	44
Bro.1	100	25.36	1.47	1-2	1	-3	4	Minor	6.4	Hart.2	16	11.98	0.25	0.5-2.5	0.8	-15	4	Moderate	50
Bro.2	100	20.65	1.33	1-2	1	-3	4	Moderate	28	Hart.3	180	20.96	1.25	0.1-0.5	0.8	-5	4	Negligible	18
Bro.3	100	21.74	1.33	2-5	0.77	-15	4	Moderate	42	Kam.1	140	11.98	0.20	0.1-0.5	1.1	-8	4	Minor	4.5
Bro.4	100	21.74	1.33	<1	0.77	-17	4	Moderate	56	Kam.2	140	19.56	2.00	0.1-0.5	1.1	-8	2	Negligible	27
Bro.5	100	42.25	1.33	2-5	1	-10	4	Negligible	28	Kam.3	30	7.33	0.25	0.5-2.5	1.1	-8	4	Moderate	27
Bro.6	100	52.63	1.33	<1	1	-3	2	Minor	37	Kam.4	30	7.33	0.25	0.5-2.5	1.1	-25	-	Large	49
Bro.7	100	23.60	1.33	1-2	0.77	-15	4	Large	56	Kam.5	30	2.44	1.00	0.5-2.5	1.1	-5	3	Minor	14
Bur.1	280	32.61	1.25	<1	1	-3	2	Negligible	165	Kli.1	200	18.34	3.00	0.1-0.5	1	-5	3	Negligible	1.2
Bur.2	280	22.44	1.25	<1	1	-5	2	Negligible	165	Kli.2	11	3.67	0.17	2.5-10	1	-13	4	Minor	6
Bur.3	280	28.99	0.75	1-2	1	-10	3	Moderate	165	Kli.3	11	3.67	0.17	2.5-10	1	-13	4	Moderate	11.4
Bur.4	280	27.17	0.48	2-5	1	-10	3	Large	165	Kli.4	200	18.34	3.00	0.1-0.5	1	-8	3	Minor	6.5
Cat.1	140	21.20	2.50	0.1	0.5	-13	3	Minor	60	Kli.5	11	3.67	0.17	2.5-10	1	-13	4	Minor	6.5
Cat.2	140	21.20	2.50	0.1	0.5	-13	1	Negligible	60	Kun.1	140	25.36	2.00	0-3	0.85	-8	3	Minor	35
Cat.3	140	21.20	2.50	0.1	0.5	-13	3	Large	60	Mac.1	18	3.62	2.00	<1	1	-13	3	Minor	1.1
Cop.1	280	20.65	0.25	0.5-2.5	0.5	-15	4	Moderate	5.7	Mac.2	9	3.62	0.50	<1	1	-13	3	Minor	1.1
Cop.10	280	9.98	1.33	0.5-2.5	1	-25	3	Extensive	650	Mac.3	9	3.62	2.00	<1	1	-13	3	Minor	2.6
Cop.11	280	20.65	0.25	0.5-2.5	0.5	-15	4	Minor	10	Mok.1	140	25.64	1.50	0.1-0.5	1	-8	2	Negligible	0.6
Cop.12	280	22.44	1.33	0.5-2.5	1	-10	3	Moderate	97	Mok.2	70	2.44	0.17	0.5-2.5	1	-17	5	Moderate	1.4
Cop.13	280	22.44	1.33	0.5-2.5	1	-15	3	Moderate	145	Mok.4	140	25.64	1.50	0.1-0.5	1	-8	2	Negligible	1.3
Cop.2	280	22.44	1.33	0.5-2.5	1	-10	3	Minor	4.7	Mok.5	140	25.64	1.50	0.1-0.5	1	-8	2	Negligible	3
Cop.3	280	22.44	1.33	0.5-2.5	1	-15	3	Moderate	14	Mok.6	70	2.44	0.17	0.5-2.5	1	-17	5	Large	20
Cop.4	280	9.98	1.33	0.5-2.5	1	-18	3	Large	34.7	Mok.8	140	25.64	1.50	0.1-0.5	1	-8	2	Negligible	2.3
Cop.5	280	9.98	1.33	0.5-2.5	1	-18	3	Extensive	76.1	Mok.9	70	2.44	0.17	0.5-2.5	1	-17	5	Extensive	180
Cop.6	280	9.98	1.33	0.5-2.5	1	-25	3	Extensive	47.1	Moo.1	18	12.47	0.50	2-5	1	-9	3	Minor	0.3
Cop.7	280	9.98	1.33	0.5-2.5	1	-18	3	Moderate	66.1	Moo.2	18	12.47	0.50	2-5	1	-9	3	Negligible	0.2
Cop.8	280	21.20	1.33	0.5-2.5	1	-8	3	Moderate	95	Moo.3	18	12.47	0.50	2-5	1	-18	5	Moderate	27
Cop.9	280	9.98	1.33	0.5-2.5	1	-18	3	Large	168	Moo.4	18	12.47	0.50	2-5	1	-18	5	Minor	17
Dar.1	140	19.17	2.00	1-2	0.84	-13	4	Minor	18	Osp.1	40	18.32	1.25	0.1-0.5	1.15	-13	4	Negligible	1.6
Dar.2	140	19.17	2.00	1-2	0.84	-13	4	Moderate	18	Osp.2	30	3.66	0.86	0.5-2.5	1.15	-20	4	Moderate	13.2
Dar.3	140	19.17	2.00	1-2	0.84	-13	4	Moderate	18	Osp.3	40	18.32	1.25	0.1-0.5	1.15	-13	4	Minor	1.9
Dar.5	140	16.21	2.00	1-2	1	-5	4	Minor	9	Osp.4	30	3.66	0.86	0.5-2.5	1.15	-13	4	Moderate	13.2
Dar.6	140	22.12	1.50	2-5	1	-	5	Large	3.5	Osp.5	40	18.32	1.25	0.1-0.5	1.15	-18	4	Negligible	2.2
Flo.1	200	21.98	2.50	0.1-0.5	0.5	-25	-	Moderate	120	Pin.1	70	2.95	1.50	2-5	1	-10	4	Minor	4.8
Flo.2	100	1.50	1.33	0.1-0.5	0.5	-25	-	Moderate	120	Pin.2	70	4.99	0.75	2-5	0.6	-14	4	Moderate	4.8
Gar.1	13	20.00	1.00	0.1-0.5	0.44	-5	3	Negligible	1	Pin.3	70	17.70	0.60	5	0.75	-10	5	Moderate	0.4
Gar.2	13	20.00	1.00	0.1-0.5	0.44	-8	-	Minor	14	Pin.4	70	9.98	0.75	2-5	1	-18	4	Large	28
Gar.4	13	20.00	1.00	0.1-0.5	0.44	-5	3	Negligible	1.3	Row.1	280	17.46	1.00	0	1	-10	4	Negligible	13
Gar.5	13	20.00	1.00	0.1-0.5	0.44	-8	-	Minor	20	Row.2	280	25.36	1.00	1-2	1	-21	4	Moderate	13
Goe.1	140	20.96	1.00	<0.1	1	-8	-	Minor	90	Spl.1	140	25.36	1.50	0-1	0.5	-3	4	Moderate	120
Goe.2	35	4.49	0.17	>10	1	-8	-	Moderate	90	Spl.2	140	37.56	1.50	0-1	0.6	-3	4	Negligible	120
Goe.3	140	20.96	1.00	<0.1	1	-8	-	Negligible	50	Spl.3	80	10.87	0.75	1-2	0.55	-3	4	Minor	24
Goe.4	35	4.49	0.17	>10	1	-8	-	Moderate	90	Way.1	140	28.99	1.50	0.1	1	-13	4	Negligible	8.6
Goe.5	35	4.49	0.17	>10	1	-8	-	Moderate	22	Way.2	140	28.99	1.50	0.1	0.8	-13	4	Negligible	8.6
Haa.1	13	5.90	0.33	2.5-10	0.48	-15	4	Large	3.6	Way.3	140	17.46	0.75	0.1	0.7	-13	4	Moderate	8.6
Haa.2	13	5.90	0.33	2.5-10	0.48	-15	4	Moderate	0.3	Way.4	35	4.99	0.25	-	1	-18	-	Moderate	22
Haa.3	13	5.90	0.33	2.5-10	0.48	-15	4	Large	3.9										